Observation of the Difference between e^--e^- and e^+-e^- Interactions

W. N. Lennard, Peter J. Schultz, G. R. Massoumi, and L. R. Logan
Department of Physics, The University of Western Ontario, London, Ontario, Canada N6A 3K7
(Received 1 July 1988)

We have measured the Au L-shell ionization-cross-section ratio for incident electrons and positrons having kinetic energies $T \simeq 25$–55 keV. In this energy region, σ_L^-/σ_L^+ is observed to be smaller than unity, reflecting the fundamental difference between the Møller and Bhabha interactions for large energy transfers. We have modified Kolbenstvedt's inner-shell ionization description to include (i) positive particles (e^+), (ii) L shells, and (iii) Coulomb-deflection effects, and find reasonable agreement with the data.

PACS numbers: 34.80.Dp, 34.50.Fa, 71.60.+z

A large number of experimental inner-shell ionization cross sections for electron impact have been measured, but there exist few corresponding studied for positrons. Through a comparison of the electron and positron cross sections, it can be hoped to observe the effect of electron exchange, particularly for kinetic energies (T) in the near-threshold region, $T/U \gtrsim 1$, where U is the ejected-electron binding energy. At these relatively low energies, the basic difference between the e^--e^- (Møller)[1] and e^+-e^- (Bhabha)[2] interactions should be most apparent. Unfortunately, this is also the energy region for which the Coulomb interaction of the incident charged projectiles with the screened target nucleus is most important. This can act to obscure the Møller-Bhabha difference.

Most of the experimental studies to date report K-shell ionization cross sections (σ_K) at sufficiently high energies that little or no difference is observed for e^+ and e^- (see, for example, Refs. 3–6). More recent results for 100–400-keV e^+ and e^- incident on Ag (Ref. 7) ($U_K \simeq 26$ keV) and 25–40-keV e^+ and e^- on Cu (Ref. 8) ($U_K \simeq 9$ keV) show that σ_K^- exceeds σ_K^+ near threshold, contrary to Møller-Bhabha scattering considerations, but consistent with Coulomb enhancement of σ_K^- relative to σ_K^+.

In order to suppress the strong influence of the nuclear Coulomb effect, we have studied L-shell ionization for e^+ and e^- incident on Au at very low energies, $2 < T/U_L < 4$, where σ_L^+ may be expected to exceed σ_L^-. Our results exhibit unambiguously a larger cross section for the positron-induced excitation, and suggest that Coulomb-interaction affects are small but not negligible. Using a simple model following Kolbenstvedt[9] to describe the Møller-Bhabha cross-section differences, and accounting for the Coulomb deflection via a semiclassical Monte Carlo calculation, we obtain good agreement with the experimental data.

The experimental geometry is shown in Fig. 1. Monoenergetic e^+ and e^- beams variable in energy from $\simeq 0$ to 60 keV were obtained from the University of Western Ontario positron beam facility.[10] A totally depleted 100-μm Si surface-barrier detector (SBD) was used to count the number of incident particles. Its 40-μg/cm^2-thick gold entrance electrode served as a suitably thin target. The target was bombarded with e^+ and e^- beams at several known energies. During the experiment, the particle rate was kept at $\simeq 3\times10^4$ counts/s for both e^- and e^+ measurements. Characteristic Au L x rays produced in the target were measured on the axis of the beam transport system through the 8-μm-thick Be window of a Kevex Si(Li) detector (30 mm$^2\times$3 mm, resolution = 170 eV at 5.9 keV). An Al filter of thickness 0.02 mm was positioned in front of the detector to attenuate Si K x rays. The Si(Li) detector was operated at $\frac{1}{3}$ the usual bias voltage to reduce its sensitivity to 511-keV annihilation γ rays. The corresponding change in efficiency for Au $L\alpha$ and $L\beta$ x radiation ($\simeq 9.7$ and 11.5 keV) was negligible. A carbon aperture of 2 mm diameter was positioned directly in front of the SBD to exclude edge regions, where incomplete charge collection can occur. A movable ^{241}Am radioactive source was positioned in front of the detector system periodically to check the x-ray calibration of the x-ray detector.

The L-shell ionization cross section σ_L can be determined from $\sigma_L = N_x\epsilon_p/N_p t\epsilon_x\omega_x$, where N_x is the number of characteristic x rays, N_p is the number of detected incident particles, t is the target thickness, ϵ_x is the absolute efficiency of the x-ray detector, ϵ_p is the absolute efficiency of the SBD, and ω_x is the average fluorescence yield for the x rays of interest. Since our goal was to determine the cross-section ratio, σ_L^-/σ_L^+, the common parameters ϵ_x, t, and ω_x cancel. A difference in the ϵ_p

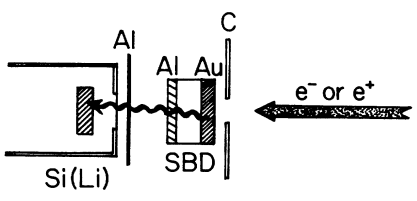

FIG. 1. Schematic diagram of the experimental arrangement in the target chamber.

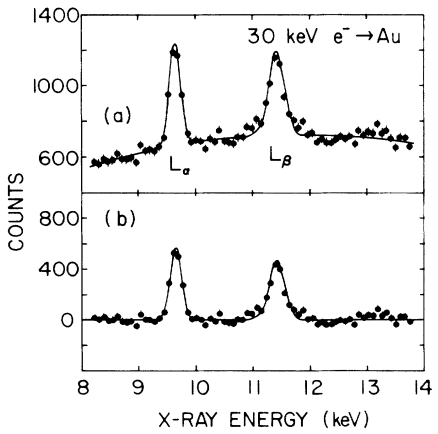

FIG. 2. Typical Au L x-ray spectrum observed with a Si(Li) detector for 30-keV incident electrons. Spectrum (a) is the raw data and (b) is the residual after subtraction of the smoothly varying continuum background. The positions of Au $L\alpha$ and $L\beta$ are indicated.

value of $<2\%$ may be anticipated as a result of e^+-e^- differences in backscattering[11]; however, we consider the experimental data to be nondefinitive on this subject,[12] and thus we assume $\epsilon_p^- = \epsilon_p^+$ in the analysis. The principal source of uncertainty arises from the difficulty in the extraction of N_x for the e^+ measurements. We have used the sum of the Au $L\alpha$ and $L\beta$ intensities in our data analysis, although analyses based on either line independently agree within the experimental error.

The e^+ and e^- particle spectra are essentially indistinguishable for identical incident energies. Typical photon spectra for both e^- and e^+ projectiles are shown in Figs. 2 and 3, respectively. For the e^+ measurements, there is a much larger background caused by the 511-keV annihilation γ rays. The decreased Si(Li) bias minimized the sensitive volume of the detector for pulses originating from this source. The sharp increase in photon yield for $E_x \leq 9$ keV evident in Fig. 3(a) was observed to move to higher E_x values for increasing Si(Li) bias, thus decreasing the signal-to-background ratio. Additionally, Compton-scattered photons with energies slightly exceeding the Au L binding energy may excite characteristic x rays via photoionization of either the Au target (i.e., the SBD entrance electrode) or the thin Au electrode on the Si(Li) detector. In order to estimate the contribution to the x-ray yields from secondary processes, a graphite plate with 20-mm diameter and 2-mm thickness was placed immediately before the SBD. The thickness of this plate was sufficient to stop all incident positrons. In this case, since the target was irradiated only by photons which include the annihilation γ rays from the plate and x rays scattered from the surroundings, any Au L x rays detected would be caused by photoionization. Moreover, by insertion of a graphite stopper, any contribution to the characteristic x-ray yield caused by projectile-induced bremsstrahlung radiation can also be determined. We conducted this test for incident e^+ and e^- fluences more than twice that accumulated during the cross-section measurements, and found no evidence for Au characteristic L x rays. We also attempted to excite Au L x rays by placing a ^{137}Cs γ-ray source ($E_\gamma = 661$ keV) immediately in front of the SBD. Here also, no discrete Au L x rays were observed above background.

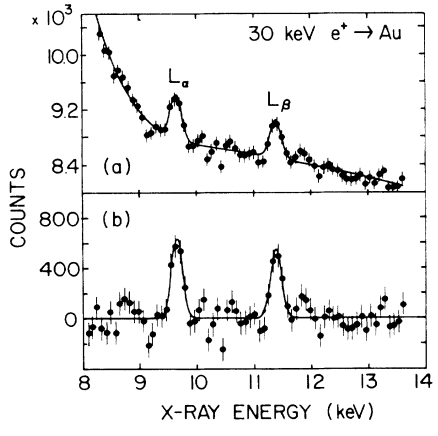

FIG. 3. Same as Fig. 2, except for 30-keV incident positrons. The increased background at low energies apparent in (a) arises from Compton scattering of the annihilation γ rays.

The measured cross-section ratios are shown in Fig. 4 for the energy region 25–55 keV, corresponding to T/U_L values in the range $\simeq 2$–4. We have taken $U_L = 12.98$ keV as a weighted average over the L_1, L_2, and L_3 shells for Au. Each datum represents a counting interval $\simeq 100$ h (i.e., $\simeq 50$ h for each e^+ and e^- energy). The dashed line is the result of a calculation following the work of Kolbenstvedt.[9] In this work, an impact-parameter description is used to divide the total cross section into separate contributions from close and distant collisions. For distant collisions, corresponding to impact parameters or b values exceeding the L-shell radius, r_L, the method of virtual quanta[13] yields a cross section via

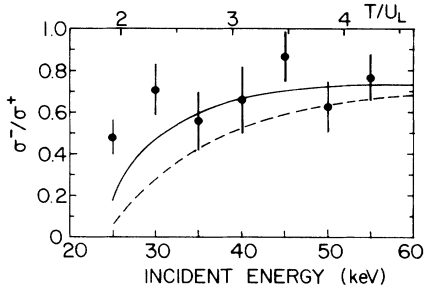

FIG. 4. Measured L-shell ionization-cross-section ratio σ_L^-/σ_L^+, for positrons and electrons incident on Au. The dashed curve shows the results obtained from the modified Kolbenstvedt calculation. The solid curve includes the Coulomb-deflection effect.

photoionization. For $b < r_L$, the Møller and Bhabha cross sections are integrated for e^--e^- and e^+-e^- collisions, respectively. The two contributions are summed to give the total cross section.

In addition to the above, it is important to include the effect of the nuclear Coulomb field on differences in the L-shell ionization probabilities for incident particles of opposite charge. The exact solution of this problem requires a formidable application of many-body collision theory. We have made an estimate of the effect for incident e^+ and e^- by considering differences in the flux distributions of the incident projectiles about the nucleus. This procedure is intended to provide an estimate for a correction that may be combined with the Kolbenstvedt-based theory to yield a better theoretical description. In this calculation, the particle trajectory in a binary collision with a nucleus is uniquely determined from a specification of the mass, charge, impact parameter, and kinetic energy of the projectile. To estimate the probability of a "collision" with an atomic L-shell electron, we evaluate the probability density for the total L-shell electron wave function along the trajectory. The details of the assignment of a volume to the particle path are unimportant since the volume elements involved in a numerical integration will cancel in the formation of the e^+/e^- ratio of such integrals. We have used hydrogenic wave functions for the Au L-shell electrons, with an effective nuclear charge $Z=70$. The results were not sensitive to this choice.

To account for the change in projectile velocity along the trajectory due to Coulomb interaction, the L-shell probability density at each point was multiplied by the generalized Gryzinski ionization cross section[14] evaluated for particles with mass m_e and the appropriate instantaneous kinetic energy. We note that the so-called Coulomb effect arises from two related phenomena: First, the e^- trajectory is on average closer to the nucleus than the e^+ trajectory; second, and by far the more important in this experiment, the Gryzinski cross section increases sharply with increasing projectile velocity in the threshold region. The latter phenomenon is analogous to the so-called energy-loss effect found for heavy-ion–induced inner-shell ionization with positively charged projectiles.[15]

The ratio of calculations for e^+ and e^- projectiles was constructed by random sampling of the impact parameters with a Monte Carlo approach, with appropriate weighting. Good convergence (within a few percent) was found after $\simeq$800 trajectories. The solid curve in Fig. 4 shows the Kolbenstvedt model (dashed curve) multiplied by the Coulomb correction factor. The agreement with our data is surprisingly good.

It is instructive to question the validity of the calculations used to derive L-shell cross-section ratios. Certainly, the Kolbenstvedt approach should not be accurate in the threshold region where it is not strictly valid to treat the ionizing process as a collision between two free particles. Our semiclassical Monte Carlo calculation assumes to first order that the Gryzinski expression for the ionization cross section applies equally to both e^+ and e^-. This assumption may not be appropriate because the influence of the nuclear Coulomb field has been ignored in that work. At high velocities such an estimate should be adequate, but less so in the threshold region. It may be that the shortcomings of the threshold descriptions are not so important when cross section ratios are formed. We believe the present agreement between experiment and calculation is not fortuitous and are presently extending the calculations to the K shell in order to compare with the Ag (Ref. 7) and Cu (Ref. 8) K x-ray data.

In summary, we have measured the Au L-shell ionization-cross-section ratio for e^- and e^+ in the near-threshold energy region ($2 \leq T/U_L \leq 4$). We observe $\sigma_L^- < \sigma_L^+$, which we interpret as evidence for the Møller-Bhabha scattering cross-section difference at large energy transfers. The experimental results are in reasonable agreement with a calculation that incorporates the Coulomb-deflection effect in a semiclassical manner, suggesting that the effect of Coulomb deflection is much reduced for these L-shell data relative to earlier K-ionization measurements. The present data constitute a challenge for future theoretical models of electron-atom and positron-atom collisions.

We are grateful for helpful discussions of this work with E. Merzbacher, P. F. A. Alkemade, K. G. Lynn, S. R. Valurri, and S. P. Goldman. This work was supported by grants from the National Sciences and Engineering Research Council, Canada (W.N.L., P.J.S.), and by research support from the Center for Chemical Physics at the University of Western Ontario.

[1]C. Møller, Ann. Phys. (Leipzig) **14**, 531 (1932)

[2]H. J. Bhabha, Proc. Roy. Soc. London A **154**, 195 (1936).

[3]S. A. H. Seif el Nasr, D. Berenyi, and Gy. Bibok, Z. Phys. **271**, 207 (1974).

[4]H. Hansen, H. Weigmann, and A. Flammersfeld, Nucl. Phys. **58**, 241 (1964).

[5]H. Hansen and A. Flammersfeld, Nucl. Phys. **79**, 135 (1966).

[6]U. Schiebel, E. Bentz, A. Müller, E. Salzborn, and H. Tawara, Phys. Lett. **59A**, 274 (1976).

[7]S. Ito, S. Shimizu, T. Kawaratani, and K. Kubota, Phys. Rev. A **22**, 407 (1980).

[8]Peter J. Schultz and John L. Campbell, Phys. Lett. **112A**, 316 (1985).

[9]H. Kolbenstvedt, J. Appl. Phys. **38**, 4785 (1967).

[10]Peter J. Schutlz, Nucl. Instrum. Methods Phys. Res., Sect. B **30**, 94 (1988).

[11]A. Bisi and L. Braicovich, Nucl. Phys. **58**, 171 (1964).

[12]W. N. Lennard, Peter J. Schultz, and G. R. Massoumi, Nucl. Instrum. Methods Phys. Res., Sect. B **33**, 128 (1988).

[13]J. D. Jackson, *Classical Electrodynamics* (Wiley, New York, 1962), Chap. 15.

[14]M. Gryzinski, Phys. Rev. **138**, A336 (1965).

[15]W. Brandt and G. Lapicki, Phys. Rev. A **23**, 1717 (1981).